



## Research Paper

# The retinal pigment epithelium in Sorsby Fundus Dystrophy shows increased sensitivity to oxidative stress-induced degeneration

Alyson Wolk<sup>a,b,1</sup>, Mala Upadhyay<sup>a,1</sup>, Mariya Ali<sup>a</sup>, Jason Suh<sup>a</sup>, Heidi Stoehr<sup>c</sup>, Vera L. Bonilha<sup>a,d</sup>, Bela Anand-Apte<sup>a,b,d,\*</sup>

<sup>a</sup> Department of Ophthalmic Research, Cole Eye Institute & Lerner Research Institute, Cleveland Clinic Foundation, 9500 Euclid Ave, Cleveland, OH, 44195, USA

<sup>b</sup> Cleveland Clinic Lerner College of Medicine, Dept. of Molecular Medicine, Case Western Reserve University, 10900 Euclid Ave, Cleveland, OH, 44106, USA

<sup>c</sup> Institute of Human Genetics, University of Regensburg, 31 Universitätsstraße, Regensburg, 93053, Germany

<sup>d</sup> Cleveland Clinic Lerner College of Medicine of Case Western Reserve University, Dept. of Ophthalmology, 10900 Euclid Ave, Cleveland, OH, 44106, USA

## ARTICLE INFO

## Keywords:

Retinal pigment epithelium  
Sorsby Fundus Dystrophy  
Age-related macular degeneration  
Oxidative stress  
Antioxidants  
Sodium iodate

## ABSTRACT

Sorsby Fundus Dystrophy (SFD) is a rare inherited autosomal dominant macular degeneration caused by specific mutations in *TIMP3*. Patients with SFD present with pathophysiology similar to the more common Age-related Macular Degeneration (AMD) and loss of vision due to both choroidal neovascularization and geographic atrophy. Previously, it has been shown that RPE degeneration in AMD is due in part to oxidative stress. We hypothesized that similar mechanisms may be at play in SFD. The objective of this study was to evaluate whether mice carrying the S179C-*Timp3* mutation, a variant commonly observed in SFD, showed increased sensitivity to oxidative stress. Antioxidant genes are increased at baseline in the RPE in SFD mouse models, but not in the retina. This suggests the presence of a pro-oxidant environment in the RPE in the presence of *Timp3* mutations. To determine if the RPE of *Timp3* mutant mice is more susceptible to degeneration when exposed to low levels of oxidative stress, mice were injected with low doses of sodium iodate. The RPE and photoreceptors in *Timp3* mutant mice degenerated at low doses of sodium iodate, which had no effect in wildtype control mice. These studies suggest that *TIMP3* mutations may result in a dysregulation of pro-oxidant—antioxidant homeostasis in the RPE, leading to RPE degeneration in SFD.

## 1. Introduction

Sorsby Fundus Dystrophy (SFD) [1] is an autosomal dominant, fully penetrant, degenerative disease of the macula [2]. SFD is manifested by symptoms of night blindness or sudden loss of visual acuity, usually in the third to fourth decades of life [3–5]. SFD is caused by specific mutations in the Tissue Inhibitor of Metalloproteinase-3 (*TIMP3*) gene [6–13]. The predominant histopathological feature in the eyes of patients with SFD are confluent, 20–30 μm thick, amorphous deposits found between the basement membrane of the retinal pigment epithelium (RPE) and the inner collagenous layer of Bruch's membrane. While SFD is a rare disease, it closely resembles the more common age-related macular degeneration (AMD) in the occurrence of drusen, choroidal neovascular membranes, and central geographic atrophy. SFD, however, differentiates itself from AMD with earlier onset of symptoms, strong

autosomal dominant inheritance pattern, and late involvement of peripheral chorio-retinal atrophy. The sub-retinal deposits in both SFD and AMD have been shown to be rich in *TIMP3* [14–16].

The identification of rare coding variants in the *TIMP3* gene when analyzing 16,144 AMD patients and 17,832 controls suggested that *TIMP3* may play a role in AMD [17]. In addition, the AMD Consortium identified the first genetic association signal specific to wet AMD near matrix metalloproteinase-9 (MMP9), a substrate for *TIMP3*. The clinical and histopathological similarities between AMD and SFD, the identification of variants in the *TIMP3* gene and matrix metalloproteinase pathway in AMD, and the observation that sub-retinal deposits in both SFD and AMD are rich in *TIMP3* [14–16,18] suggest that similar downstream effectors might be in play in both conditions.

Produced constitutively by the RPE [2,19], *TIMP3* is a normal component of Bruch's membrane [20], which binds to sulfated

\* Corresponding author. Department of Ophthalmic Research, Cole Eye Institute & Lerner Research Institute, Cleveland Clinic Foundation, 9500 Euclid Ave, Cleveland, OH, 44195, USA.

E-mail address: [anandab@ccf.org](mailto:anandab@ccf.org) (B. Anand-Apte).

<sup>1</sup> Co-first authors.

<https://doi.org/10.1016/j.redox.2020.101681>

Received 12 June 2020; Received in revised form 27 July 2020; Accepted 5 August 2020

Available online 10 August 2020

2213-2317/© 2020 Published by Elsevier B.V. This is an open access article under the CC BY-NC-ND license (<http://creativecommons.org/licenses/by-nc-nd/4.0/>).

glycosaminoglycans of the extracellular matrix [21,22]. While mice expressing S179C-*Timp3* (one of the mutations identified in SFD patients), showed only slight abnormalities in the inner aspect of Bruch's membrane and RPE microvilli [23] there was a clear absence of typical SFD-related pathology in mutant mice on a C57Bl/6 background. One possibility that has been suggested to explain this discrepancy between humans and mice is that the SFD-*TIMP3* mutation predisposes the retina or RPE/choroid to be more vulnerable to environmental or epigenetic stress, which may be absent in the inbred mouse strain housed under controlled conditions of the vivarium. We have recently reported that SFD mutant mice are more susceptible to laser-induced choroidal neovascularization [24]. The purpose of this study is to investigate whether mice carrying the S179C-*Timp3* mutation are more susceptible to RPE damage induced by NaIO<sub>3</sub>, an oxidizing agent that has been widely used as a model for AMD as it induces oxidative stress and subsequent damage exclusively in the RPE [25,26].

## 2. Materials and methods

### 2.1. Mice

All mice utilized in this study were housed in the Cole Eye Institute vivarium under approved Institutional Animal Care and Use Committee (IACUC) protocols. All procedures on the mice were in accordance with the ARVO Statement for the Use of Animals in Ophthalmic and Vision Research and conformed to the National Institutes of Health Guide for the Care and Use of Animals in Research. Heterozygous breeding of *Timp3*<sup>+/-S179C</sup> [23] produced homozygous *Timp3*<sup>S179C/S179C</sup> mice and age-matched, wildtype littermate controls on a C57Bl/6J background. Experiments were carried out in 4 month-old, homozygous *Timp3*<sup>S179C/S179C</sup> mice. Mice were injected via tail vein with a 1% solution (w/v) of NaIO<sub>3</sub> (Sigma-Aldrich, #71702, St. Louis, MO, USA) or PBS (control) and euthanized seven days later.

### 2.2. Isolation of RNA

Eyes were enucleated following euthanasia and immediately dissected. Retinas were removed, immediately frozen, and stored at -80 °C until use. RPE was dissociated as previously described [27]. Both eye cups (without retinas) from the same mouse were combined and incubated with RNAlater Cell Reagent (Qiagen, Hilden, Germany) for 10 min at room temperature with occasional agitation in order to dissociate the RPE from the choroid and sclera. The choroid/sclera was removed with forceps and the RPE cells were pelleted by centrifugation. Cells and tissue were lysed and RNA was extracted using the RNeasy Mini Kit (Qiagen, Hilden, Germany). Isolated RNA was treated with DNase (Invitrogen/Thermo Scientific, WA, USA) to ensure removal of all genomic DNA.

### 2.3. Quantitative PCR

250 ng of total RNA from RPE and 500 ng of total RNA from retina were converted into cDNA using Verso cDNA kit (Thermo Scientific, WA, USA). Quantitative PCR was performed using Radiant Green HI-ROX qPCR Kit (Alkali Scientific LLC, Fort Lauderdale, FL, USA). Relative fold change was determined using 2<sup>-ΔΔCt</sup> method. For all analyses, *Gapdh* was used as internal control. For analysis of retina and RPE markers, obtained Ct values were normalized to values from retina samples (Fig. 1). For relative gene expression assays, obtained Ct values were normalized to values from WT littermate controls (Fig. 2). Below is the description of primer sequences used:

*Nrf2*—Forward:5'-GATGAGGATGGAAAGCCTTAC-3',  
Reverse:5'-TAGCTCAGAAAAGGCTCCATC-3';  
*Sod1*—Forward:5'-GAACCATCCACTTCGAGCA-3',  
Reverse: 5-TACTGATGGACGTGGAACCC-3';  
*Sod2*—Forward:5'-ACTGAAGTTCAATGGTGGGG-3',

Reverse: 5'-GCTTGATAGCCTCCAGCAAC-3';  
*DJ-1/Park7*—Forward: 5'-CTACGGCTCTGTTGGCTCAC-3',  
Reverse: 5'-GCGGCTCTCTGAGTAGCTGTA-3';  
*Rhod*—Forward: 5'-CCCTTCTCCAACGTCACAGG-3',  
Reverse: 5'-TGAGGAAGTTGATGGGGAAGC-3';  
*Rpe65*—Forward: 5'-AAGCTGCATATCTCTCGTTC-3',  
Reverse: 5'-TGGGAATTGAACACACGATCTG-3';  
*Gapdh*—Forward:5'-CGTCCCGTAGACAAAATGGT-3',  
Reverse: 5'- TTGATGGCAACAATCTCCAC-3'.

### 2.4. Western blotting and quantifications

Eyes were enucleated immediately after euthanasia and immediately dissected to remove anterior segment and retina. Both eye cups (without retinas) from the same mouse were placed in the same tube with RIPA buffer (Alfa Aesar, Haverhill, MA, USA) + protease/phosphatase inhibitors (Sigma Aldrich, St. Louis, MO, USA) and incubated on ice for 30 min with agitation every 5 min to dissociate the RPE from the choroid/sclera. After incubation, the choroid/sclera was removed from the tube and RPE was lysed by passing through 27 ½ G needle and syringe. Lysates were clarified by centrifugation. Protein content was quantified in each lysate using the Micro BCA Protein Assay Kit (Thermo Scientific, WA, USA). Western blots were performed as previously described [28]. The protein levels were quantified using Image Studio V5.2 software (LI-COR Biosciences, Lincoln, NE, USA). The following antibodies were used: β-actin—(mouse monoclonal IgG, #8H10D10, Cell Signaling Technology, Danvers, MA, USA); DJ-1—(Rabbit polyclonal IgG, #NB300-270, Novus Biologicals, Littleton, CO, USA); Sod1—(Mouse monoclonal IgG, #SC-101523, Santa Cruz Biotechnology, Dallas, TX, USA).

### 2.5. Plastic sections and bright field imaging

After euthanasia, the dorsal side of the eyes were labeled for orientation and the eyes subsequently enucleated. Whole eyes were immediately placed in cold fixative solution (2% PFA (Electron Microscopy Sciences, Hatfield, PA, USA), 2.5% glutaraldehyde (Polysciences, Warrington, PA, USA), 0.1 M sodium cacodylate (Electron Microscopy Sciences, Hatfield, PA, USA), 0.00111% calcium chloride (Millipore Sigma, Burlington, MA, USA)). After initial fixation, incisions were made just below the limbus and the eyes were then returned to fixative for the duration of the incubation. After fixation, the anterior segment, lens, and vitreous were dissected away from the posterior eye cups. The eye cups were washed with cold 0.1 M sodium cacodylate, post-fixed in osmium tetroxide (Electron Microscopy Sciences, Hatfield, PA, USA) (1% OsO<sub>4</sub>, 0.1 M sodium cacodylate), and washed again in 0.1 M sodium cacodylate. The eye cups were dehydrated by incubating them in sequentially increasing concentrations of cold ethanol, infiltrated with propylene oxide (Thermo Fisher Scientific, Waltham, MA, USA), and embedded in epon. Resin blocks were cut into 0.75 μm sections and stained with toluidine blue (Thermo Fisher Scientific, #T161, Waltham, MA, USA). Sections were imaged with Zeiss Axioimager. Z1 using MRc5 camera (Zeiss, Oberkochen, Germany) at 40X.

### 2.6. Flat mounts, imaging, and quantification of RPE degeneration

Enucleated eyes were fixed in 4% paraformaldehyde (Electron Microscopy Sciences, Hatfield, PA, USA), after which retinas were mechanically detached from the RPE/choroid under a dissecting microscope. The flat mounts with exposed RPE were then processed for labeling with phalloidin-TRITC (1:1000; Sigma-Aldrich, #P1951, St. Louis, MO, USA) as previously described [29]. RPE/choroid flat mounts were mounted on glass slides and images were acquired using a laser scanning confocal microscope (TCS-SP8, Leica, Wetzlar, Germany). Serial Z-stacks and tiles of the flat-mounted RPE were collected and merged into a three-dimensional projection of the entire flat-mount.

Images were acquired using identical settings. Quantification of RPE degeneration was calculated using ImageJ2 [30]. Micrographs were calibrated from a reference scale embedded in the image. Quantifications were performed as previously described [28]. Briefly, the outline of the whole RPE/choroid area and of the degenerated area were delineated using the freehand line tool in ImageJ2. In cases where not all areas of degeneration were contiguous, separate areas of degeneration were summed to determine the cumulative area of degeneration. This area was divided by the total area of the flat-mounted RPE to determine percent degeneration. The edges of degenerated area were defined as regions in which the RPE cells are present but their morphology is not the typical hexagonal shape as shown by TRITC-phalloidin staining.

## 2.7. Statistical analysis

All data were analyzed using GraphPad Prism v7.0 (GraphPad Software, La Jolla, CA, USA). All data were normally distributed and are presented as mean  $\pm$  SEM. Groups for qPCR were compared using unpaired, two-tailed Student's *t*-test. Similarly, comparisons of RPE degeneration within groups was performed using unpaired, two-tailed Student's *t*-test. Significance threshold ( $\alpha$ ) was set to 0.05.

## 3. Results

### 3.1. The RPE has increased expression of antioxidant genes in mice carrying the *S179C-Timp3* mutation

To evaluate the expression of antioxidant genes in the retina and RPE, eyes from 4-month old, homozygous *S179C-Timp3* mice and wildtype (WT) littermate mice were enucleated and RNA was isolated from retinas and RPE for expression analysis. To ensure contaminant-free isolation of RNA from each tissue, relative enrichment of retina and RPE marker genes were analyzed. *RPE65* is exclusively expressed by RPE [31] and in our samples was approximately 70-fold enriched in RNA from RPE compared to RNA isolated from retinas (Fig. 1A). Similarly, rhodopsin (*Rhod*) is expressed predominantly in photoreceptors [32] and was found to be enriched approximately 3-fold in retina RNA isolations compared to RPE RNA isolations (Fig. 1B).

Next, the expression of four major antioxidant genes was analyzed in the RPE from age-matched *S179C-Timp3* mice and WT controls from at least 4 male and 4 female mice ( $n = 8$  total) from each group. *Nrf2*, *Park7* (more commonly referred to as DJ-1), *Sod1*, and *Sod2* have previously been characterized to be upregulated in response to oxidative stress [33–36]. *Nrf2* (Fig. 2A), *Park7* (DJ-1) (Fig. 2B), *Sod1* (Fig. 2C), and *Sod2* (Fig. 2D) genes were upregulated at least 2 fold in RPE from *S179C-Timp3* mice compared to WT controls (Fig. 2). However, there are no changes in the expression of *Sod1* and DJ-1 at the protein level in WT

or *S179C-Timp3* mice (Supplemental Fig. 1).

In contrast, the retina showed no significant changes in antioxidant gene expression (*Nrf2* (Fig. 3A), *Park7* (Fig. 3B), *Sod1* (Fig. 3C), and *Sod2* (Fig. 3D)) between *S179C-Timp3* mice and WT controls (Fig. 3). This suggests that there may be a RPE-specific oxidative stress in SFD or that oxidative stress response is an integral part of a typical RPE reaction to diseases or pathology.

### 3.2. Mice carrying *S179C-Timp3* mutation are more susceptible to $\text{NaIO}_3$ -induced retinal degeneration

Due to increased expression of antioxidant genes in *S179C-Timp3* mice, we hypothesized that the RPE of *S179C-Timp3* mice would be more susceptible to damage from low levels of oxidative stress. Sodium iodate has been widely used as a model for oxidative stress-induced RPE degeneration [37–43].

To evaluate the relative susceptibility of mice carrying the *S179C-Timp3* mutation to RPE degeneration, WT and *S179C-Timp3* mice were injected intravenously with either low dose (10 mg/kg body weight) or high dose (20 mg/kg body weight)  $\text{NaIO}_3$ . One week after injection, the eyes of experimental mice were evaluated by histology (Fig. 4). Both WT and *S179C-Timp3* groups had normal retinas with PBS control injections (Fig. 4A–a, F–f). Upon injection with low dose of  $\text{NaIO}_3$ , retinas from WT mice remained intact (Fig. 4B–b, C–c) while retinas from *S179C-Timp3* mice began showing signs of RPE degeneration and disorganization of the outer nuclear layer (Fig. 4G–g, H–h). At high doses of  $\text{NaIO}_3$ , both WT and *S179C-Timp3* mice had severe degeneration of the RPE and outer retina (Fig. 4D–d, E–e, I–i, J–j). This indicates that WT mice are still susceptible to damage from oxidative stress as induced by  $\text{NaIO}_3$ , but much more oxidative stress is required in order to see degeneration comparable to that of *S179C-Timp3* mice at low doses.

#### 3.2.1. *S179C-Timp3* mice have increased area of RPE degeneration induced by $\text{NaIO}_3$

To analyze the effect of  $\text{NaIO}_3$  specifically on the RPE, RPE/choroid flat mounts of experimental mice were analyzed for degeneration after staining with rhodamine-phalloidin, a reagent that binds filamentous actin (Fig. 5). As before, two doses of  $\text{NaIO}_3$  were used (10 mg/kg and 20 mg/kg) and one week passed between injection and enucleation. Both WT and *S179C-Timp3* mice injected with PBS had normal RPE morphology (Fig. 5A–a, D–d). However, after injection with low dose of  $\text{NaIO}_3$ , degeneration began in the central region of the RPE of *S179C-Timp3* mice (Fig. 5E–e) while no degeneration occurred in the RPE of WT mice (Fig. 5B–b). Both WT and *S179C-Timp3* mice had severe loss of RPE after injection with high doses of  $\text{NaIO}_3$  (Fig. 5C–c, F–f).

The area of degeneration was centralized around the optic nerve and was quantified as percent of total area of the flat mount (Fig. 5G). These

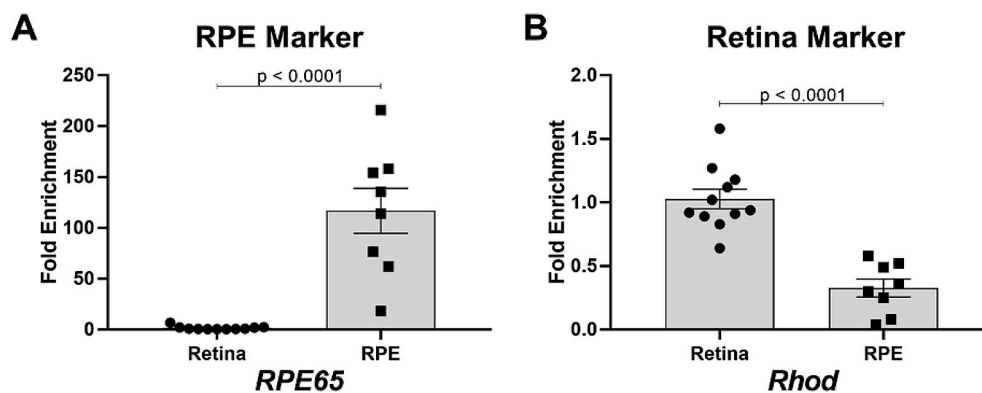
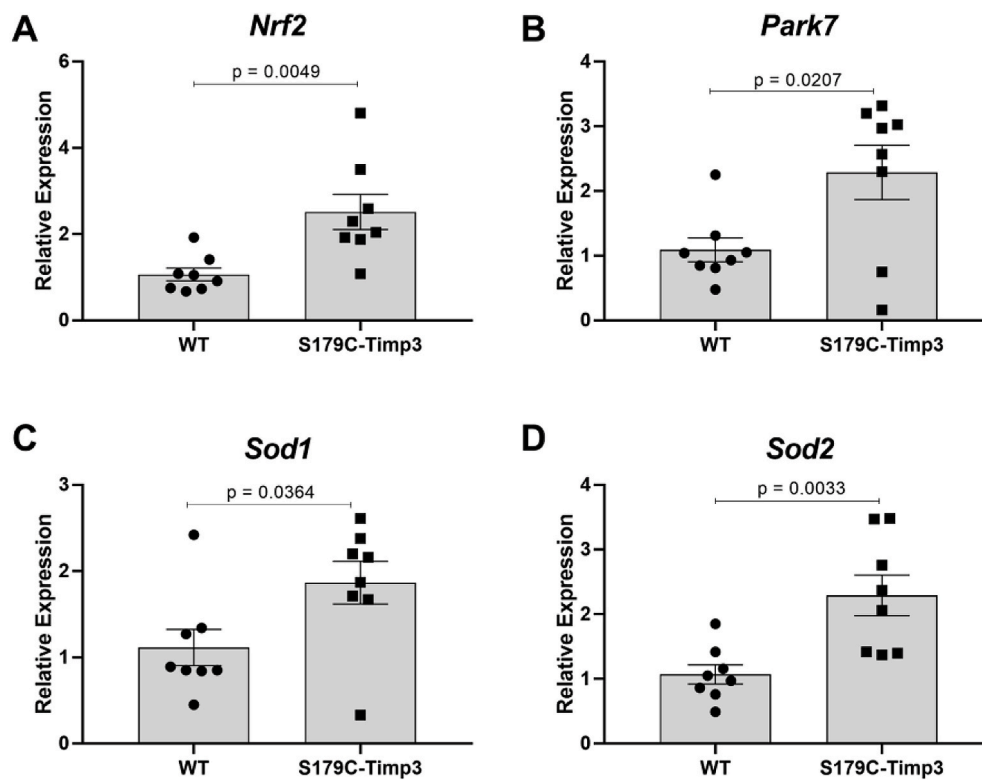
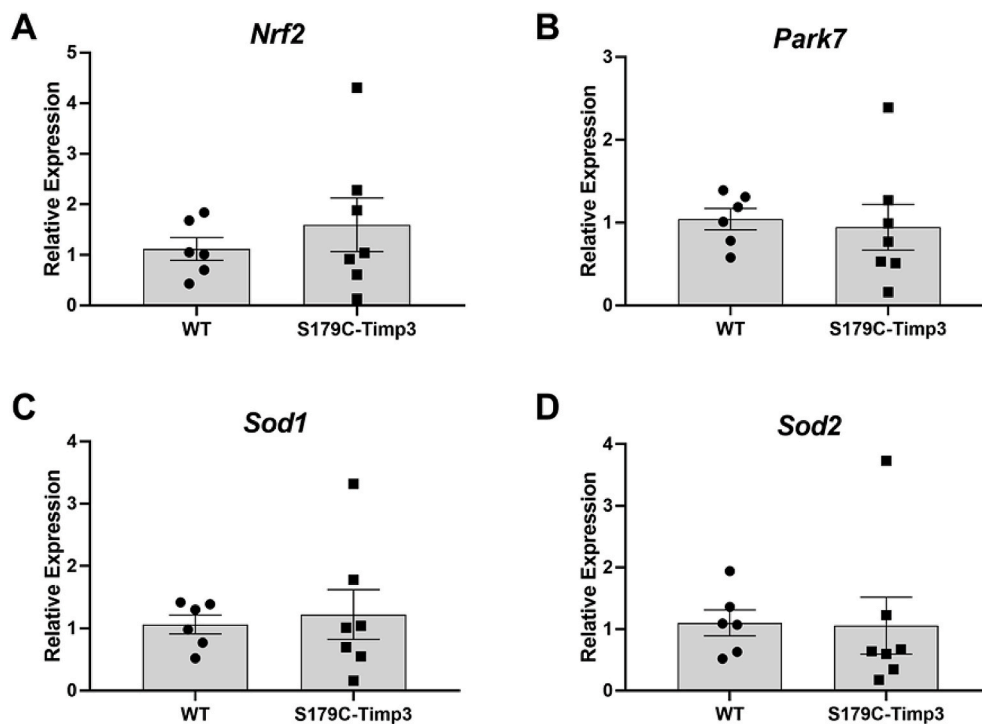


Fig. 1. RNA isolated from retina and RPE shows enrichment in marker genes specific for each tissue. A) *RPE65* was enriched in RNA extracted from RPE compared to RNA extracted from retinas. B) *Rhod* was enriched in RNA extracted from retinas compared to RNA extracted from RPE. A–B) Fold changes are shown relative to retina. Comparisons were analyzed using Student's unpaired *t*-test.  $n > 8$  for each analysis.



**Fig. 2.** Antioxidant gene expression is increased in RPE from S179C-Timp3 mice. A) *Nrf2*, B) *Park7*, C) *Sod1*, and D) *Sod2* were analyzed by quantitative PCR using RNA extracted from RPE from S179C-Timp3 mice and WT littermate controls. A-D) Fold changes are shown relative to WT samples. Comparisons were analyzed using Student's unpaired *t*-test.  $n = 8$  for each analysis.



**Fig. 3.** Antioxidant gene expression is unaltered in retina from S179C-Timp3 mice. A) *Nrf2*, B) *Park7*, C) *Sod1*, and D) *Sod2* were analyzed by quantitative PCR using RNA extracted from retinas from S179C-TIMP3 mice and WT littermate controls. A-D) Fold changes are shown relative to WT samples. Comparisons were analyzed using Student's unpaired *t*-test.  $n = 8$  for each analysis.

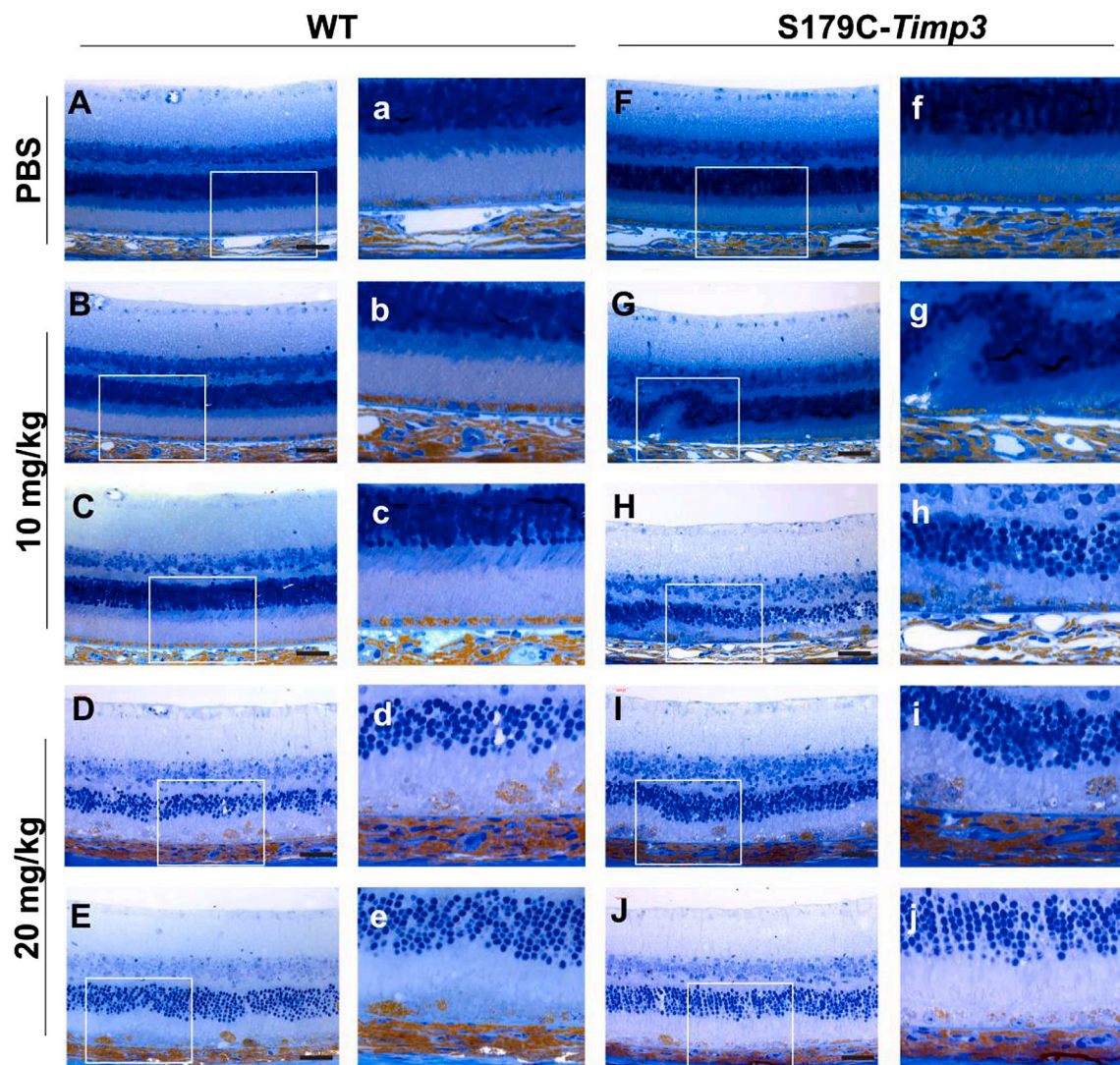


**Fig. 4.** *S179C-Timp3* mice have increased degeneration of RPE and outer retina after injection with low doses of sodium iodate. Plastic sections of WT (A-E) and *S179C-Timp3* (F-J) mice show varying levels of degeneration after injections with NaIO<sub>3</sub>. n > 3 for each group. Whole-retina images taken at 40x (A-J) and magnified images from insets (a-j) showing degeneration of RPE and photoreceptors. A-a, F-f) Sections from mice injected with PBS only had no degeneration. G-g, H-h) *S179C-Timp3* mice injected with 10 mg/kg NaIO<sub>3</sub> showed degeneration of the RPE and outer retina, but WT mice with the same dose did not (B-b, C-c). D-d, E-e, I-i, J-j) Both WT and *S179C-Timp3* mice had severe degeneration after injection with 20 mg/kg NaIO<sub>3</sub>. Black scale bars in images represent 40  $\mu$ m.

areas of degeneration were defined as cells that deviated from the normal hexagonal morphology by becoming larger, elongated cells with stress fibers detected by TRITC-phalloidin (Fig. 5C-c, E-e, F-f, arrowheads). Areas without any TRITC-phalloidin staining were indicative of complete loss of RPE (Fig. 5C-c, E-e, F-f asterisks). There was no significant difference in area of degeneration between WT and *S179C-Timp3* mice given high doses of NaIO<sub>3</sub> (Fig. 5G, right). However, there was a significant increase in area of RPE degeneration in *S179C-Timp3* mice after injection with low dose of NaIO<sub>3</sub> (Fig. 5G, middle).

#### 4. Discussion

Oxidation-reduction (redox) homeostasis plays a critical role in a number of physiological processes. The concept of oxidative stress was first proposed in 1985 as “a disturbance in the prooxidant-antioxidant balance in favor of the former” [44] and subsequently, the regulation of redox signaling has been the subject of intense investigation [45–47]. Oxidative stress has been hypothesized to play an important role in the pathogenesis of a number of retinal dystrophies including AMD [48]. Many studies have suggested that the severe RPE degeneration in

geographic atrophy is a consequence of a loss of antioxidant functions [49–54]. Whether oxidative stress is a factor in the pathogenesis of Sorsby Fundus Dystrophy has not been investigated prior to this study.

The RPE, which constitutes the outer blood-retinal barrier, sits as a monolayer of cuboidal, polarized pigmented cells on Bruch’s membrane, between the choroid and the neural retina. In addition to its barrier function, the RPE is involved in retinoid storage and metabolism and provides the machinery for phagocytosis of the outer segments of photoreceptors. The RPE is highly metabolically active and exposed to high levels of oxygen and age-pigment, such as lipofuscin, which makes it increasingly susceptible to oxidative stress.

A number of molecular redox switches have been identified that control redox signaling and/or redox sensing [44]. Nuclear Factor-E2-related Factor 2 (Nrf2) belongs to a small family of redox sensitive transcription factors that has been postulated to be a key defensive mechanism against oxidative stress [55]. Four key antioxidant genes were analyzed in this study: *Nrf2*, *Park7/DJ-1* [29,56], *Sod1*, and *Sod2* [57]. We found increased antioxidant gene expression in the RPE (Fig. 2), but not in the retina (Fig. 3) of *S179C-Timp3* mice at baseline. While we did not see significant changes at the protein level

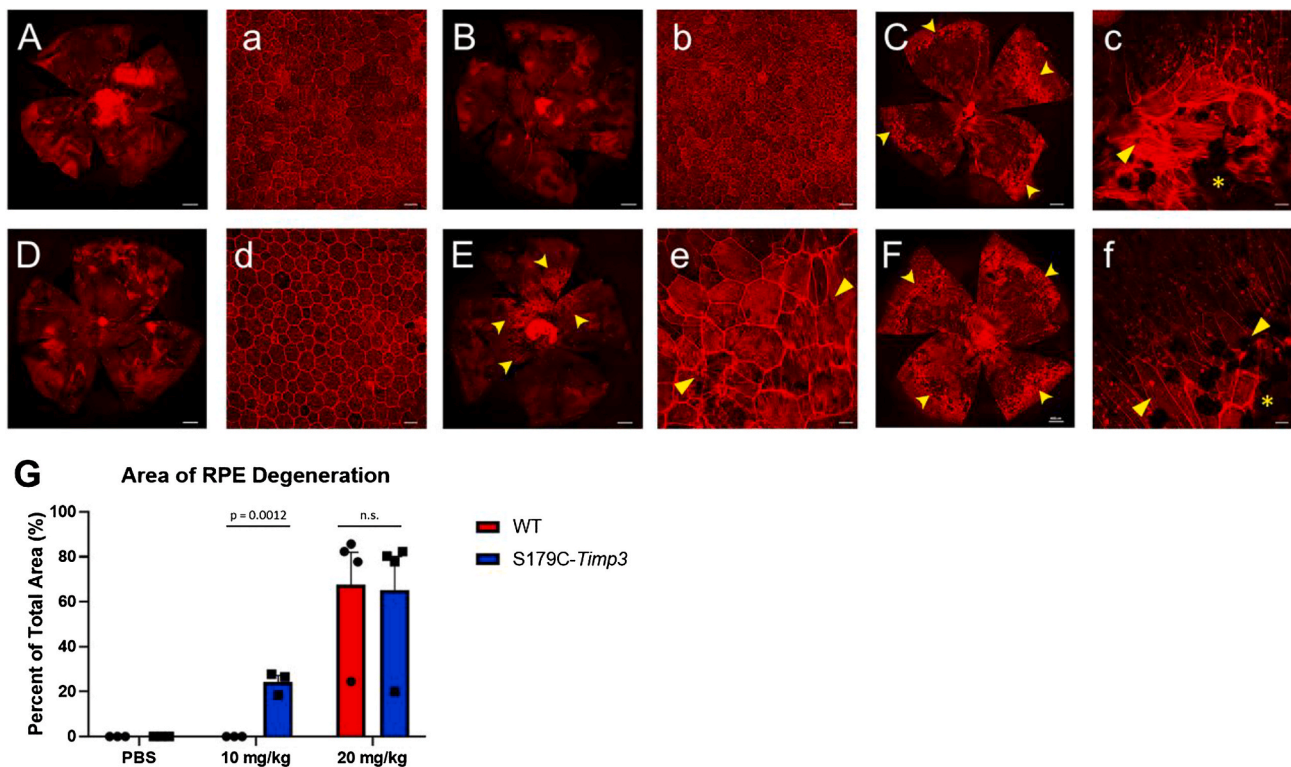


**Fig. 5.** *S179C-Timp3* mice have increased area of RPE degeneration after injections with low doses of sodium iodate. **A, a-C, c)** RPE/choroid flat mounts of WT and *S179C-Timp3* (**Dd-Ff**) mice show varying levels of degeneration after injections with  $\text{NaIO}_3$ .  $n > 3$  for each group. **A, B, C, D, E, F)** Tile scan images of flat mounts stained with TRITC-phalloidin. White scale bars represent 400  $\mu\text{m}$  **a, b, c, d, e, f)** Higher magnification images of each flat mount showing RPE morphology and areas of cell death. White scale bars represent 45  $\mu\text{m}$ . **A-a, D-d)** Flat mounts from mice injected with PBS only had no degeneration. **E-e)** *S179C-Timp3* mice injected with 10 mg/kg  $\text{NaIO}_3$  had degeneration of the RPE and areas of elongated cells with stress fibers (**arrowheads**), but WT mice with the same dose did not (**B-b**). **C-c, F-f)** Both WT and *S179C-Timp3* mice had severe degeneration (**asterisks**) and cell morphology changes (**arrowheads**) after injection with 20 mg/kg  $\text{NaIO}_3$ . **G)** Area of RPE degeneration was quantified as percent of total area of the flat mount. Student's unpaired t-tests were used to analyze comparisons within each treatment group.

(Supplemental Fig. 1), the increase at the mRNA level remains a critical observation because it suggests that oxidative stress sensing mechanisms are at play in the RPE of *S179C-Timp3* mice. Moreover, studies have shown that mRNA levels do not always correlate to protein levels in post-mitotic cells, such as RPE [58]. Lack of correlation between mRNA and protein has been reported in many systems and ascribed to a number of mechanisms including post-transcriptional mechanisms, half-life of proteins, protein degradation, etc [59]. Together, these data suggest that in SFD, the RPE is the initial target of oxidative stress, and by extension, the initial target of disease. This is not surprising as *TIMP3* has previously been shown to be expressed primarily in the RPE and choroid [2]. The observation of increased antioxidant gene expression in the RPE of SFD mice also suggests that the presence of mutant *Timp3* likely creates a pro-oxidant environment in the RPE. Whether this is caused by an MMP-dependent or -independent pathway has yet to be determined. We cannot rule out the possibility that the antioxidant machinery (at least the ones we tested: *Nrf2*, *DJ-1*, *Sod1*, and *Sod2*) may be working appropriately in SFD, but that under identical baseline oxidative stress conditions, wildtype mice may simply generate a more robust antioxidant response. However, our data suggest specific RPE sensitivity to oxidative stress that are unique to the *S179C-Timp3* mice. This will be the focus of future studies as we have yet to identify the pro-oxidant pathways at play in SFD.

We hypothesize that the baseline pro-oxidant environment of the RPE in *S179C-Timp3* mice render them more susceptible to low levels of oxidative stress. This was seen in the development of pathological changes in the RPE of mutant mice exposed to low doses of  $\text{NaIO}_3$ . There was a significant loss of RPE and photoreceptors one week after injection with low doses of  $\text{NaIO}_3$  in the mutant mice but not in WT mice, as

shown by histology (Figs. 4 and 5). The area of RPE degeneration after injection with low dose of  $\text{NaIO}_3$  in *S179C-Timp3* mice (Fig. 5) consistently began in the central retina adjacent to the optic nerve and spread outwards, likely due to the intravenous delivery of  $\text{NaIO}_3$ . Bordering the areas of RPE loss, the RPE was elongated with filamentous actin stress fibers, suggesting that RPE stress precedes cell death (Fig. 5, arrowheads), similar to what has been hypothesized to occur in geographic atrophy in AMD.

The idea that patients with AMD have a chronic low level oxidative stress in their retinas has led to the proposal of antioxidant therapy as a treatment for AMD [60]. Supplementation with vitamin A, a potent antioxidant, is often prescribed for AMD patients [61, 62][61, 62]. Our study points to the possibility of antioxidant therapy being potentially beneficial for patients with SFD. Future studies will investigate if antioxidant therapy mitigates RPE degeneration due to oxidative stress in *S179C-Timp3* mice.

#### Declaration of competing interest

The authors declare that they have no known competing financial interests or personal relationships that could have appeared to influence the work reported in this paper.

#### Acknowledgements

This work was supported in part by US National Institute of Health EY027083 (BA-A), EY026181 (BA-A), EY027750 (VLB), P30EY025585 (BA-A), T32EY024236 (AW), Research to Prevent Blindness (RPB) Challenge Grant and RPB Lew Wasserman award to BA-A, Cleveland Eye

Bank Foundation and funds from Cleveland Clinic Foundation. We thank Sujata Rao and her laboratory for kindly sharing their rhodopsin qPCR primer sequences. We wish to extend a sincere apology to colleagues whose work was not cited due to space limitations.

## Appendix A. Supplementary data

Supplementary data to this article can be found online at <https://doi.org/10.1016/j.redox.2020.101681>.

## References

- [1] A. Sorsby, M.E. Joll Mason, A fundus dystrophy with unusual features, *Br. J. Ophthalmol.* (1949) 67–97.
- [2] N.G. Della, P.A. Campochiaro, D.J. Zack, Localization of TIMP-3 mRNA expression to the retinal pigment epithelium, *Invest. Ophthalmol. Vis. Sci.* 37 (9) (1996) 1921–1924.
- [3] S.G. Jacobson, A.V. Cideciyan, G. Regunath, F.J. Rodriguez, K. Vandenberg, V. C. Sheffield, E.M. Stone, Night blindness in Sorsby's fundus dystrophy reversed by vitamin A, *Nat. Genet.* 11 (1) (1995) 27–32.
- [4] H. Kalmus, D. Seedburgh, Probable common origin of a hereditary fundus dystrophy (Sorsby's familial pseudo inflammatory macular dystrophy) in an English and Australian family, *J. Med. Genet.* 13 (4) (1976) 271–276.
- [5] P.J. Polkinghorne, M.R. Capon, T. Berninger, A.L. Lyness, K. Sehmi, A.C. Bird, Sorsby's fundus dystrophy. A clinical study, *Ophthalmology* 96 (12) (1989) 1763–1768.
- [6] I.A. Barbazetto, M. Hayashi, C.M. Klais, L.A. Yannuzzi, R. Allikmets, A novel TIMP3 mutation associated with Sorsby fundus dystrophy, *Arch. Ophthalmol.* 123 (4) (2005) 542–543.
- [7] U. Felbor, C. Benkwitz, M.L. Klein, J. Greenberg, C.Y. Gregory, B.H. Weber, Sorsby fundus dystrophy: reevaluation of variable expressivity in patients carrying a TIMP3 founder mutation, *Arch. Ophthalmol.* 115 (12) (1997) 1569–1571.
- [8] U. Felbor, H. Stohr, T. Amann, U. Schonherr, B.H. Weber, A novel Ser156Cys mutation in the tissue inhibitor of metalloproteinases-3 (TIMP3) in Sorsby's fundus dystrophy with unusual clinical features, *Hum. Mol. Genet.* 4 (12) (1995) 2415–2416.
- [9] K.P. Langton, M.D. Barker, N. McKie, Localization of the functional domains of human tissue inhibitor of metalloproteinases-3 and the effects of a Sorsby's fundus dystrophy mutation, *J. Biol. Chem.* 273 (27) (1998) 16778–16781.
- [10] K.P. Langton, N. McKie, A. Curtis, J.A. Goodship, P.M. Bond, M.D. Barker, M. Clarke, A novel tissue inhibitor of metalloproteinases-3 mutation reveals a common molecular phenotype in Sorsby's fundus dystrophy, *J. Biol. Chem.* 275 (35) (2000) 27027–27031.
- [11] R.J. Lin, M.S. Blumenkranz, J. Binkley, K. Wu, D. Vollrath, A novel His158Arg mutation in TIMP3 causes a late-onset form of Sorsby fundus dystrophy, *Am. J. Ophthalmol.* 142 (5) (2006) 839–848.
- [12] Y. Tabata, Y. Isashiki, K. Kamimura, K. Nakao, N. Ohba, A novel splice site mutation in the tissue inhibitor of the metalloproteinases-3 gene in Sorsby's fundus dystrophy with unusual clinical features, *Hum. Genet.* 103 (2) (1998) 179–182.
- [13] B.H. Weber, G. Vogt, R.C. Pruett, H. Stohr, U. Felbor, Mutations in the tissue inhibitor of metalloproteinase-3 (TIMP-3) in patients with Sorsby's fundus dystrophy, *Nat. Genet.* 8 (1994) 352–356.
- [14] R.N. Fariss, S.S. Apte, P.J. Luthert, A.C. Bird, A.H. Milam, Accumulation of tissue inhibitor of metalloproteinases-3 in human eyes with Sorsby's fundus dystrophy or retinitis pigmentosa, *Br. J. Ophthalmol.* 82 (11) (1998) 1329–1334.
- [15] M. Kamei, S.S. Apte, M.E. Rayborn, H. Lewis, J.G. Hollyfield, TIMP-3 accumulation in drusen and Bruch's membrane in eyes from donors with age-related macular degeneration, in: M.M. Luvail, R.E. Anderson, J.G. Hollyfield (Eds.), *Degenerative Diseases of the Retina*, Plenum Press, New York, 1997, pp. 11–15, 1997.
- [16] J.H. Qi, G. Dai, P. Luthert, S. Chaurasia, J. Hollyfield, B.H. Weber, H. Stohr, B. Anand-Apte, S156C mutation in tissue inhibitor of metalloproteinases-3 induces increased angiogenesis, *J. Biol. Chem.* 284 (30) (2009) 19927–19936.
- [17] L.G. Fritsche, W. Igl, J.N. Bailey, F. Grassmann, S. Sengupta, J.L. Bragg-Gresham, K.P. Burdon, S.J. Hebburn, C. Wen, M. Gorski, I.K. Kim, D. Cho, D. Zack, E. Souied, H.P. Scholl, E. Bala, K.E. Lee, D.J. Hunter, R.J. Sardell, P. Mitchell, J.E. Merriam, V. Cipriani, J.D. Hoffman, T. Schick, Y.T. Lechanteur, R.H. Guymer, M.P. Johnson, Y. Jiang, C.M. Stanton, G.H. Buitendijk, X. Zhan, A.M. Kwong, A. Bolea, M. Brooks, L. Gieser, R. Ratnapriya, K.E. Branham, J.R. Forster, J.R. Heckenlively, M.I. Othman, B.J. Vote, H.H. Liang, E. Souzeau, I.L. McAllister, T. Isaacs, J. Hall, S. Lake, D.A. Mackey, L.J. Constable, J.E. Craig, T.E. Kitchner, Z. Yang, Z. Su, H. Luo, D. Chen, H. Ouyang, K. Flagg, D. Lin, G. Mao, H. Ferreyra, K. Stark, C. N. von Strachwitz, A. Wolf, C. Brandl, G. Rudolph, M. Olden, M.A. Morrison, D. J. Morgan, M. Schu, J. Ahn, G. Silvestri, E.E. Tsironi, K.H. Park, L.A. Farrer, A. Orlin, A. Brucker, M. Li, C.A. Curcio, S. Mohand-Said, J.A. Sahel, I. Audo, M. Benchaboune, A.J. Cree, C.A. Rennie, S.V. Goverdhan, M. Grunin, S. Hagbi-Levi, P. Campochiaro, N. Katsanis, F.G. Holz, F. Blond, H. Blanche, J.F. Deleuze, R. P. Igo Jr., B. Truit, N.S. Peachey, S.M. Meuer, C.E. Myers, E.L. Moore, R. Klein, M. A. Hauser, E.A. Postel, M.D. Courtenay, S.G. Schwartz, J.L. Kovach, W.K. Scott, G. Liew, A.G. Tan, B. Gopinath, J.C. Merriam, R.T. Smith, J.C. Khan, H. Shahid, A. T. Moore, J.A. McGrath, R. Laux, M.A. Brantley Jr., A. Agarwal, L. Ersoy, A. Caramoy, T. Langmann, N.T. Saksens, E.K. de Jong, C.B. Hoyng, M.S. Cain, A. J. Richardson, T.M. Martin, J. Blangero, D.E. Weeks, B. Dhillon, C.M. van Duijn, K. F. Doheny, J. Romm, C.C. Klaver, C. Hayward, M.B. Gorin, M.L. Klein, P.N. Baird, A.I. den Hollander, S. Fauser, J.R. Yates, R. Allikmets, J.J. Wang, D.A. Schaumberg, B.E. Klein, S.A. Hagstrom, I. Chowers, A.J. Lotery, T. Leveillard, K. Zhang, M. H. Brilliant, A.W. Hewitt, A. Swaroop, E.Y. Chew, M.A. Pericak-Vance, M. DeAngelis, D. Stambolian, J.L. Haines, S.K. Iyengar, B.H. Weber, G.R. Abecasis, I.M. Heid, A large genome-wide association study of age-related macular degeneration highlights contributions of rare and common variants, *Nat. Genet.* 48 (2) (2016), 134–43.
- [18] J.W. Crabb, M. Miyagi, X. Gu, K. Shadrach, K.A. West, H. Sakaguchi, M. Kamei, A. Hasan, L. Yan, M.E. Rayborn, R.G. Salomon, J.G. Hollyfield, Drusen proteome analysis: an approach to the etiology of age-related macular degeneration, *Proc. Natl. Acad. Sci. U. S. A.* 99 (23) (2002) 14682–14687.
- [19] J.H. Qi, Q. Ebrahem, K. Yeow, D.R. Edwards, P.L. Fox, B. Anand-Apte, Expression of Sorsby's fundus dystrophy mutations in human retinal pigment epithelial cells reduces matrix metalloproteinase inhibition and may promote angiogenesis, *J. Biol. Chem.* 30 (2002) 30.
- [20] R.N. Fariss, S.S. Apte, B.R. Olsen, K. Iwata, A.H. Milam, Tissue inhibitor of metalloproteinases-3 is a component of Bruch's membrane of the eye, *Am. J. Pathol.* 150 (1) (1997) 323–328.
- [21] L. Troeberg, C. Lazenbatt, E.K.M.F. Anower, C. Freeman, O. Federov, H. Habuchi, O. Habuchi, K. Kimata, H. Nagase, Sulfated glycosaminoglycans control the extracellular trafficking and the activity of the metalloproteinase inhibitor TIMP-3, *Chem. Biol.* 21 (10) (2014) 1300–1309.
- [22] W.H. Yu, S. Yu, Q. Meng, K. Brew, J.F. Woessner Jr., TIMP-3 binds to sulfated glycosaminoglycans of the extracellular matrix, *J. Biol. Chem.* 275 (40) (2000) 31226–31232.
- [23] B.H. Weber, B. Lin, K. White, K. Kohler, G. Soboleva, S. Herterich, M.W. Seeliger, G.B. Jaissle, C. Grimm, C. Reme, A. Wenzel, E. Asan, H. Schrewe, A mouse model for Sorsby fundus dystrophy, *Invest. Ophthalmol. Vis. Sci.* 43 (8) (2002) 2732–2740.
- [24] J.H. Qi, B. Bell, R. Singh, J. Batoki, A. Wolk, A. Cutler, N. Prayson, M. Ali, H. Stohr, B. Anand-Apte, Sorsby fundus dystrophy mutation in tissue inhibitor of metalloproteinase 3 (TIMP3) promotes choroidal neovascularization via a fibroblast growth factor-dependent mechanism, *Sci. Rep.* 9 (1) (2019) 17429.
- [25] J. Hanus, C. Anderson, D. Sarraf, J. Ma, S. Wang, Retinal pigment epithelial cell necroptosis in response to sodium iodate, *Cell death discovery* 2 (2016), 16054.
- [26] R. Kannan, D.R. Hinton, Sodium iodate induced retinal degeneration: new insights from an old model, *Neural regeneration research* 9 (23) (2014) 2044–2045.
- [27] C. Xin-Zhao Wang, K. Zhang, B. Aredeo, H. Lu, R.L. Ufret-Vincenty, Novel method for the rapid isolation of RPE cells specifically for RNA extraction and analysis, *Exp. Eye Res.* 102 (2012) 1–9.
- [28] M. Upadhyay, C. Milliner, B. Bell, V.L. Bonilha, Oxidative Stress in the Retina and Retinal Pigment Epithelium (RPE): Role of Aging and DJ-1, *Redox Biology in Press*, 2020.
- [29] V.L. Bonilha, B.A. Bell, M.E. Rayborn, I.S. Samuels, A. King, J.G. Hollyfield, C. Xie, H. Cai, Absence of DJ-1 causes age-related retinal abnormalities in association with increased oxidative stress, *Free Radic. Biol. Med.* 104 (2017) 226–237.
- [30] C.T. Rueden, J. Schindelin, M.C. Hiner, B.E. DeZonia, A.E. Walter, E.T. Arena, K. W. Elliceiri, ImageJ2: ImageJ for the next generation of scientific image data, *BMC Bioinf.* 18 (1) (2017) 529.
- [31] A. Nicoletti, D.J. Wong, K. Kawase, L.H. Gibson, T.L. Yang-Feng, J.E. Richards, D. A. Thompson, Molecular characterization of the human gene encoding an abundant 61 kDa protein specific to the retinal pigment epithelium, *Hum. Mol. Genet.* 4 (4) (1995) 641–649.
- [32] J.F. McGinnis, P.J. Leveille, A biomolecular approach to the study of the expression of specific genes in the retina, *J. Neurosci. Res.* 16 (1) (1986) 157–165.
- [33] B. Huang, J.J. Liang, X. Zhuang, S.W. Chen, T.K. Ng, H. Chen, Intravitreal Injection of Hydrogen Peroxide Induces Acute Retinal Degeneration, Apoptosis, and Oxidative Stress in Mice, *Oxidative Medicine and Cellular Longevity* 2018, 5489476.
- [34] M. Kamoshita, E. Toda, H. Osada, T. Narimatsu, S. Kobayashi, K. Tsubota, Y. Ozawa, Lutein acts via multiple antioxidant pathways in the photo-stressed retina, *Sci. Rep.* 6 (2016), 30226.
- [35] J. Martín-Nieto, M.L. Uribe, J. Esteve-Rudd, M.T. Herrero, L. Campello, A role for DJ-1 against oxidative stress in the mammalian retina, *Neurosci. Lett.* 708 (2019), 134361.
- [36] Y. Shao, H. Yu, Y. Yang, M. Li, L. Hang, X. Xu, A Solid Dispersion of Quercetin Shows Enhanced Nrf2 Activation and Protective Effects against Oxidative Injury in a Mouse Model of Dry Age-Related Macular Degeneration, *Oxidative Medicine and Cellular Longevity* 2019, 2019, 1479571.
- [37] I.A. Bhattu, S. Ogura, R. Baldeosingh, D.S. McLeod, G.A. Luty, M.M. Edwards, An acute injury model for the phenotypic characteristics of geographic atrophy, *Invest. Ophthalmol. Vis. Sci.* 59 (4) (2018) Amd143–amd151.
- [38] G. Chowers, M. Cohen, D. Marks-Ohana, S. Stika, A. Eijzenberg, E. Banin, A. Obolensky, Course of sodium iodate-induced retinal degeneration in albino and pigmented mice, *Invest. Ophthalmol. Vis. Sci.* 58 (4) (2017) 2239–2249.
- [39] Q. Jian, Z. Tao, Y. Li, Z.Q. Yin, Acute retinal injury and the relationship between nerve growth factor, Notch1 transcription and short-lived dedifferentiation transient changes of mammalian Muller cells, *Vis. Res.* 110 (Pt A) (2015) 107–117.
- [40] A. Machalinska, M.P. Kawa, E. Pius-Sadowska, D. Roginska, P. Klos, B. Baumert, B. Wiszniewska, B. Machalinski, Endogenous regeneration of damaged retinal pigment epithelium following low dose sodium iodate administration: an insight into the role of glial cells in retinal repair, *Exp. Eye Res.* 112 (2013) 68–78.
- [41] A. Machalinska, R. Lejkowska, M. Duchnik, M. Kawa, D. Roginska, B. Wiszniewska, B. Machalinski, Dose-dependent retinal changes following sodium iodate administration: application of spectral-domain optical coherence tomography for

- monitoring of retinal injury and endogenous regeneration, *Curr. Eye Res.* 39 (10) (2014) 1033–1041.
- [42] A. Machalinska, W. Lubinski, P. Klos, M. Kawa, B. Baumert, K. Penkala, R. Grzegorzolka, D. Karczewicz, B. Wiszniewska, B. Machalinski, Sodium iodate selectively injures the posterior pole of the retina in a dose-dependent manner: morphological and electrophysiological study, *Neurochem. Res.* 35 (11) (2010) 1819–1827.
- [43] Y. Yang, T.K. Ng, C. Ye, Y.W. Yip, K. Law, S.O. Chan, C.P. Pang, Assessing sodium iodate-induced outer retinal changes in rats using confocal scanning laser ophthalmoscopy and optical coherence tomography, *Invest. Ophthalmol. Vis. Sci.* 55 (3) (2014) 1696–1705.
- [44] H. Sies, *Oxidative Stress*, Academic, London, 1985.
- [45] H. Sies, Oxidative stress: a concept in redox biology and medicine, *Redox biology* 4 (2015) 180–183.
- [46] H. Sies, C. Berndt, D.P. Jones, Oxidative stress, *Annu. Rev. Biochem.* 86 (2017) 715–748.
- [47] H. Sies, D.P. Jones, Reactive oxygen species (ROS) as pleiotropic physiological signalling agents, *Nat. Rev. Mol. Cell Biol.* 21 (7) (2020) 363–383.
- [48] B.D. E, G. Marfany, The relevance of oxidative stress in the pathogenesis and therapy of retinal dystrophies, *Antioxidants* 9 (4) (2020).
- [49] E.E. Brown, A.J. DeWeerd, C.J. Ildefonso, A.S. Lewin, J.D. Ash, Mitochondrial oxidative stress in the retinal pigment epithelium (RPE) led to metabolic dysfunction in both the RPE and retinal photoreceptors, *Redox biology* 24 (2019), 101201.
- [50] S. Datta, M. Cano, K. Ebrahimi, L. Wang, J.T. Handa, The impact of oxidative stress and inflammation on RPE degeneration in non-neovascular AMD, *Prog. Retin. Eye Res.* 60 (2017) 201–218.
- [51] L. Donato, R. D'Angelo, S. Alibrandi, C. Rinaldi, A. Sidoti, C. Scimone, Effects of A2E-induced oxidative stress on retinal epithelial cells: new insights on differential gene response and retinal dystrophies, *Antioxidants* 9 (4) (2020).
- [52] J. Hanus, C. Anderson, S. Wang, RPE necroptosis in response to oxidative stress and in AMD, *Ageing Res. Rev.* 24 (Pt B) (2015) 286–298.
- [53] K. Kaarniranta, H. Uusitalo, J. Blasiak, S. Felszeghy, R. Kannan, A. Kauppinen, A. Salminen, D. Sinha, D. Ferrington, Mechanisms of mitochondrial dysfunction and their impact on age-related macular degeneration, *Prog. Retin. Eye Res.* (2020), 100858.
- [54] S.K. Mitter, C. Song, X. Qi, H. Mao, H. Rao, D. Akin, A. Lewin, M. Grant, W. Dunn Jr., J. Ding, C. Bowes Rickman, M. Boulton, Dysregulated autophagy in the RPE is associated with increased susceptibility to oxidative stress and AMD, *Autophagy* 10 (11) (2014) 1989–2005.
- [55] K. Itoh, T. Chiba, S. Takahashi, T. Ishii, K. Igarashi, Y. Katoh, T. Oyake, N. Hayashi, K. Satoh, I. Hatayama, M. Yamamoto, Y. Nabeshima, An Nrf2/small Maf heterodimer mediates the induction of phase II detoxifying enzyme genes through antioxidant response elements, *Biochem. Biophys. Res. Commun.* 236 (2) (1997) 313–322.
- [56] V.L. Bonilha, Oxidative stress regulation and DJ-1 function in the retinal pigment epithelium: implications for AMD, *Adv. Exp. Med. Biol.* 1074 (2018) 3–9.
- [57] G. Bresciani, I.B. da Cruz, J. Gonzalez-Gallego, Manganese superoxide dismutase and oxidative stress modulation, *Adv. Clin. Chem.* 68 (2015) 87–130.
- [58] K. Perl, K. Ushakov, Y. Pozniak, O. Yizhar-Barnea, Y. Bhonker, S. Shivatzki, T. Geiger, K.B. Avraham, R. Shamir, Reduced changes in protein compared to mRNA levels across non-proliferating tissues, *BMC Genom.* 18 (1) (2017) 305.
- [59] D. Greenbaum, C. Colangelo, K. Williams, M. Gerstein, Comparing protein abundance and mRNA expression levels on a genomic scale, *Genome Biol.* 4 (9) (2003) 117.
- [60] M.R. Biswal, P. Han, P. Zhu, Z. Wang, H. Li, C.J. Ildefonso, A.S. Lewin, Timing of antioxidant gene therapy: implications for treating dry AMD, *Invest. Ophthalmol. Vis. Sci.* 58 (2) (2017) 1237–1245.
- [61] M. Eggersdorfer, A. Wyss, Carotenoids in human nutrition and health, *Arch. Biochem. Biophys.* 652 (2018) 18–26.
- [62] J.R. Sparrow, Vitamin A-aldehyde adducts: AMD risk and targeted therapeutics, *Proc. Natl. Acad. Sci. U. S. A.* 113 (17) (2016) 4564–4569.